

# Characterization of conichalcite by SEM, FTIR, Raman and electronic reflectance spectroscopy

B. J. REDDY, R. L. FROST\* AND W. N. MARTENS

Inorganic Materials Research Program, Queensland University of Technology, 2 George Street, Brisbane, GPO Box 2434, Queensland 4001, Australia

## ABSTRACT

The mineral conichalcite from the western part of Bagdad mine, Bagdad, Eureka District, Yavapai County, Arizona, USA has been characterized by electronic, near-infrared (NIR), Raman and infrared (IR) spectroscopy. Scanning electron microscopy (SEM) images show that the mineral consists of bundles of fibres. Calculations based on the results of the energy dispersive X-ray analyses on a stoichiometric basis show the substitution of arsenate by 12 wt.% of phosphate in the mineral. Raman and IR bands are assigned in terms of the fundamental modes of  $\text{AsO}_4^{3-}$  and  $\text{PO}_4^{3-}$  molecules and are related to the mineral structure. Near-IR reflectance spectroscopy shows the presence of adsorbed water and hydroxyl units in the mineral. The Cu(II) coordination polyhedron in conichalcite can have at best pseudo-tetragonal geometry. The crystal field and tetragonal field parameters of the Cu(II) complex were calculated and found to agree well with the values reported for known tetragonal distortion octahedral complexes.

**KEYWORDS:** conichalcite, adelite, austenite, duftite, SEM and EDX analyses, FTIR, Raman spectroscopy, electronic reflectance spectroscopy.

## Introduction

CONICALCALCITE,  $\text{CaCuAsO}_4\text{OH}$ , forms in the oxidation zone of copper ore bodies. It is a member of the adelite group of minerals which also includes such species as austenite, adelite and duftite. In general, members of the group have the formula  $AB^{2+}(XO_4)(OH)$  where cation  $A$  may be Ca or Pb and cation  $B$  may be Zn, Mg, Fe, Co, Ni, Cu or selected combinations of these atoms and  $X$  is  $\text{As}^{5+}$  or  $\text{P}^{5+}$ . These isostructural minerals crystallize in the orthorhombic space group  $P2_12_12_1$ .

The crystal structure of conichalcite was first determined by Qurashi and Barnes (1963) originally in  $Pnma$  with final refinement in  $P2_12_12_1$ . Later it was refined by Radcliffe and Simmons (1971) with unit-cell parameters,  $a = 0.7393$ ,  $b = 0.9220$  and  $c = 0.5830$  nm. The

structure of conichalcite consists of a three-dimensional assemblage of distorted  $\text{AsO}_4$  tetrahedra,  $\text{CuO}_4(\text{OH})_2$  tetragonal bipyramids and  $\text{CaO}_7(\text{OH})$  square antiprisms, sharing corners and edges.

Available chemical data show the formation of solid solutions between austenite and conichalcite (Jambor *et al.*, 1980; Taggart and Foord, 1980; Keller *et al.*, 1981, 1982). A complete solid solution also exists between conichalcite and duftite (Jambor *et al.*, 1980).

The Raman spectra of tetrahedral anions in aqueous systems are well known. For the arsenate anion, the symmetric stretching vibration ( $\nu_1$ ) occurs at  $810\text{ cm}^{-1}$  which coincides with the asymmetric stretching mode ( $\nu_3$ ). The two bending modes ( $\nu_2$ ) and ( $\nu_4$ ) are observed at 342 and at  $398\text{ cm}^{-1}$ , respectively (Frost *et al.*, 2002, 2003*b*; Martens *et al.*, 2003*a,c*, 2004; Frost and Weier, 2004*b*). Of all the spectra for tetrahedral oxyanions, the positions of the arsenate vibrations occur at lower wavenumbers than any of the other naturally occurring mineral oxyanion spectra.

\* E-mail: r.frost@qut.edu.au

DOI: 10.1180/0026461056920243

Several spectra of arsenates including the basic copper arsenates olivenite and euchroite were reported by Farmer (1974) but no examples of the adelite group of minerals (including conichalcite) were shown. The IR spectra of the minerals conichalcite, austinite, olivenite and adamite have been reported (Sumin De Portilla, 1974). Recent studies have been carried out on arsenate minerals (Frost *et al.*, 2002, 2003*b*; Martens *et al.*, 2003*a,c*, 2004; Frost and Weier, 2004*b*).

If the point symmetry of the arsenate group is lower than the ideal tetrahedral symmetry ( $T_d$ ) then the degeneracies will be broken and splitting of the Raman bands will occur. In the adelite group the point symmetry of the arsenate group is  $C_1$  and the factor-group analysis predicts that 18 distinct Raman active modes will occur. Spectroscopic studies of the adelite group of minerals have been limited, although a Raman study of the adelite group including an Australian conichalcite has been published (Martens *et al.*, 2003*b*). In this study we examine conichalcite from a different locality (Bagdad Mine, Arizona) by Raman, Fourier transform infrared (FTIR) spectroscopy and also by electronic reflectance spectroscopy with a view to correlating the spectral behaviour with the known structure of the mineral.

The electronic spectral studies were not carried out with the specific aim of examining the effects of cations and their symmetry on any of these minerals. It would be quite interesting to study the electronic spectra of the divalent copper that is present in conichalcite. The most common electronic process revealed in the spectra of minerals is due to unfilled electron shells of transition elements and Fe is the most common transition element in minerals. The  $d^9$  configuration makes Cu(II) subject to Jahn-Teller distortion if placed in an environment of cubic (i.e. regular octahedral or tetrahedral) symmetry, and this has a profound effect on all its stereochemistry. The Cu(II) is never observed in regular environments and is usually subject to distortion. The typical distortion is an elongation along one four-fold axis, so that there is a planar array of four short Cu–L bonds and two *trans* long ones. There are numerous cases in which apparently octahedral Cu(II) complexes execute a dynamic (pulsating) Jahn-Teller behaviour, where the direction of the elongation varies rapidly. Since spectral properties vary from one mineral to another due to variation in structure and composition (Burns, 1970), the present study focuses on a conichalcite

( $CaCuAsO_4OH$ ) from Bagdad mine. Results are given in the present paper of comprehensive investigations of vibrational spectra, including Raman and IR along with the electronic spectra, and are explained in terms of the structure of anions and cations in the mineral.

## Experimental

### Samples

The conichalcite used in this study was a grass green-coloured mineral, from the personal collection of one of the authors (RLF). It originated from the western part of Bagdad mine, Arizona. The mineral was made into powder and used for the study of electronic reflectance spectroscopy in the UV-Vis region.

### Scanning electron microscopy

Scanning electron microscopes were employed for both EDXA (Joel 840 electron probe microanalyser) and secondary electron imaging (Joel 35CF). Samples for analysis were prepared by embedding in araldite, polishing with diamond paste on a Lamplan polishing cloth with water as the lubricant and coated with carbon.

### Raman microprobe spectroscopy

A small conichalcite crystal of  $\sim 1 \text{ mm}^2$  was fixed and oriented on the stage of an Olympus BHSM microscope, equipped with  $10\times$  and  $50\times$  objectives and part of a Renishaw 1000 Raman microscope system, which also includes a monochromator, a filter system and a Charge coupled Device (CCD). Raman spectra were excited by a HeNe laser (633 nm) at a resolution of  $2 \text{ cm}^{-1}$  in the range  $100\text{--}4000 \text{ cm}^{-1}$ . Repeated acquisition using the highest magnification was accumulated to improve the signal-to-noise ratio. Spectra were calibrated using the  $520.5 \text{ cm}^{-1}$  line of a silicon wafer. In order to ensure that the correct spectra are obtained, the incident excitation light was scrambled. Details of the experimental technique were reported previously (Frost *et al.*, 2002, 2003*b*, 2004; Martens *et al.*, 2003*a,c*, 2004; Frost, 2004*a,b*).

### IR and NIR spectroscopy

The IR spectrum was obtained using a Nicolet Nexus 870 FTIR spectrometer with a Smart Endurance single-bounce diamond ATR cell.

The spectrum was obtained over the 4000–500  $\text{cm}^{-1}$  region by the co-addition of 64 scans with a resolution of 4  $\text{cm}^{-1}$  and a mirror velocity of 0.6329  $\text{cm/s}$ . The NIR spectrum was collected on a Nicolet Nexus FTIR spectrometer fitted with a Nicolet Near-IR Fibreport accessory. A white light source was employed with a quartz beam splitter and TEC NIR InGaAs detector. Spectra were obtained from 11000 to 4000  $\text{cm}^{-1}$  by the co-addition of 64 scans at the resolution of 8  $\text{cm}^{-1}$ . A mirror velocity of 1.2659  $\text{m/s}$  was used. The spectra were transformed using the Kubelka-Munk algorithm for comparison with that of absorption spectra. Spectral manipulations such as baseline adjustment, smoothing and normalization were performed using the Spectralcalc software package GRAMS (Galactic Industries Corporation, NH, USA). Band component analysis was undertaken using the Jandel 'peakfit' software package which enabled the type of fitting function to be selected and allows specific parameters to be fixed or varied accordingly. Band fitting was done using a Lorentz-Gauss cross-product function with the minimum number of component bands used for the fitting process. The Lorentz-Gauss ratio was maintained at values  $>0.7$  and fitting was undertaken until reproducible results were obtained with squared correlations of  $r^2 >0.995$ .

## UV-Vis spectroscopy

UV-Vis spectroscopy is an ideal tool for the study of coloured minerals containing transition metals. Spectra of d–d transitions mainly fall in this region and can be studied either by absorption or by reflection. The technique of reflectance spectroscopy is most suitable for minerals including dark coloured and or non-transparent materials. Reflectance spectroscopy is the study of light as a function of wavelength that has been reflected or scattered from a solid, liquid or gas. As photons enter a mineral, some are reflected from grain surfaces, some pass through the grain, and some are absorbed. Those photons reflected from grain surfaces or refracted through a particle are said to be scattered. Scattered photons may encounter another grain or be scattered away from the surface so they may be detected and measured. The variety of absorption processes and their wavelength dependence allow us to derive information about the chemistry of a mineral from its reflected light. Use of the reflectance spectro-

scopy technique is growing rapidly and can be used to derive significant information about mineralogy and with little or no sample preparation. A Varian Cary 3 UV-Visible spectrophotometer, equipped with Diffuse Reflectance Accessory (DRA) was employed to record the electronic spectra of the samples in the region between 200 and 900 nm. This technique allows the study of the reflectance spectra of the samples in powder form. The DRA consists of a 73 mm diameter integrating sphere, featuring an inbuilt high-performance photomultiplier. The sample was mounted on coarse filter paper (#1) by resuspending the sample and submerging the filter paper into the suspension. Initially a base line was recorded using two pressed polytetrafluoroethylene disks (PTFE) as reference disks. Next, the sample was mounted flat over the sample port and the reflectance spectrum of the sample, relative to the reference disks, was collected by the integrating sphere. By placing the sample flat, any specular components of reflectance should be directed out of the DRA entrance port, as the angle of incidence is  $0^\circ$ . The diffuse reflectance measurements were converted into absorption (arbitrary units) using the Kubelka-Munk function ( $f(R_\infty) = (1 - R_\infty)^2 / 2R_\infty$ ). Data manipulation was performed using Microsoft Excel<sup>®</sup>.

## Results and discussion

### SEM analysis of conicalcrite

Images of conicalcrite taken at a number of magnifications are shown in Fig. 1. The figure clearly shows parallel aggregates of fibres that are pseudomorphing crystals which appear as bundles of thin prismatic crystals. The peaks of the EDX spectrum have been deconvoluted and calibrated to produce the analyses given in Table 1 which

TABLE 1. EDX analyses of conicalcrite crystals.

Atom	Wt.%			
	Grain 1	Grain 2	Grain 3	Grain 4
O	34.08	34.91	26.67	42.35
Si	0.52	1.05	0.89	0
As	25.01	23.75	27.72	21.47
P	0.93	0.93	0.76	1.23
Ca	13.09	13.24	14.62	13.18
Cu	26.37	26.13	29.33	21.76

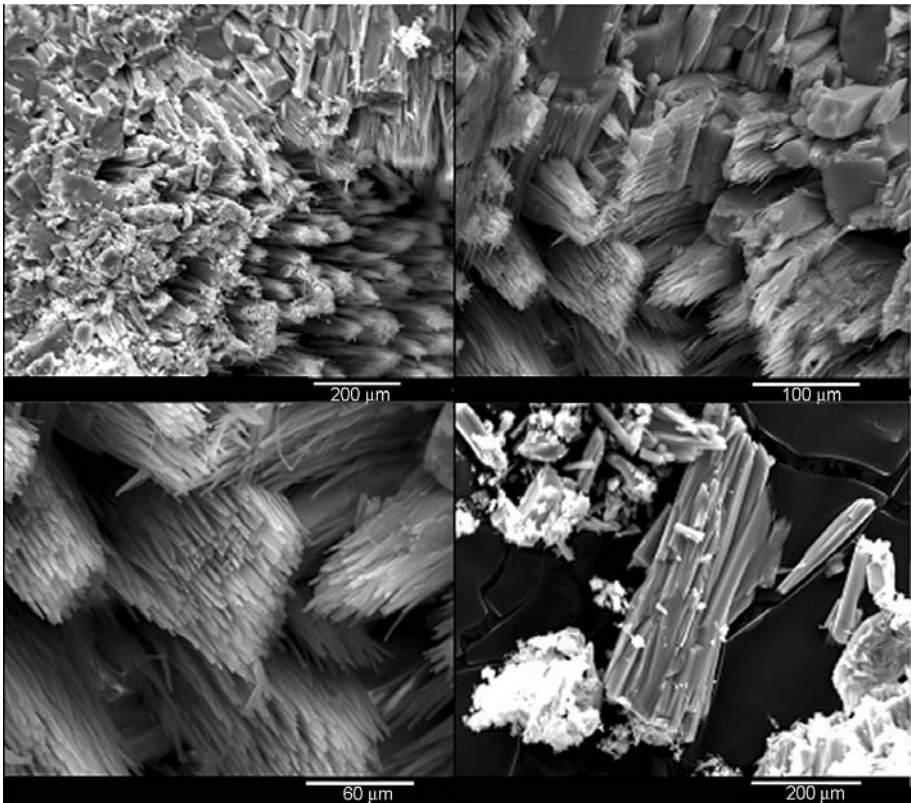


FIG. 1. SEM images of conicalcrite crystals.

show that the conicalcrite contains some isomorphous substitution of phosphate for arsenate. The amount of substitution is 12 mol.%. Thus, the chemical formula for conicalcrite is  $[(CaCu^{2+}(AsO_4)_{0.88}(PO_4)_{0.12}(OH)]$ .

#### Vibrational analysis

##### Factor group analysis

The adelite group of minerals is isostructural and exhibits  $P2_12_12_1$  symmetry. Hence the factor-group analysis is the same for all the minerals in this family. Factor group analysis yields 36 internal modes for the arsenate ion and 69 lattice vibrations in conicalcrite, with  $\Gamma = 27A + 26B_1 + 26B_2 + 26B_3$ . The theoretical vibrational analysis of conicalcrite is shown in Tables 2 and 3. The  $A_1$  symmetry of the free ion gives rise to four bands for the arsenate ion in the conicalcrite crystal with  $A, B_1, B_2, B_3$  symmetry. This implies there are four vibrations, which are Raman active. The  $A$  modes are Raman active and the  $B$  modes

are both Raman and IR active. The  $T_2$  symmetry of the free ion provides four bands for the arsenate ion in the conicalcrite crystal with  $A, B_1, B_2, B_3$  symmetry. The  $\nu_3$  mode ( $T_2$ ) splits up into three components under site symmetry  $C_1$ ; thus four anions in the unit cell give  $4 \times 3 \nu_3$  vibrations distributed into the four symmetry species of  $222-D_2'$ . This means that there are 12 antisymmetric vibrations, which should be Raman active. The free arsenate ion has tetrahedral symmetry and thus should have four bands of which two are IR active with values of  $\nu_3$  ( $T_2$ )  $887\text{ cm}^{-1}$  and  $\nu_4$  ( $T_2$ )  $463\text{ cm}^{-1}$ . The Raman active modes are observed at  $837$  ( $A_1$ ) and  $349$  ( $E$ )  $\text{cm}^{-1}$  (Farmer, 1974).

##### Vibrational spectra

The spectral features observed both in Raman and IR spectra of the conicalcrite can be divided into four regions as follows: (1) hydroxyl stretching ( $3800-2600\text{ cm}^{-1}$ ); (2) mid-IR (MIR) region

## CHARACTERIZATION OF CONICHALCITE

TABLE 2. Vibrational analysis of the internal modes of the anions in the unit cell in conichalcite.

Free ion	Site	Crystal
$T_d$	$C_1$	$D_2$
$A_1$ $E$ $2T_2$	$9A$	$9A$ $9B_1$ $9B_2$ $9B_3$

(2200–1200  $\text{cm}^{-1}$ ); (3)  $(\text{AsO}_4)^{3-}$  and  $(\text{PO}_4)^{3-}$  stretching (1100–700  $\text{cm}^{-1}$ ), and (4) low-wavenumber region,  $(\text{AsO}_4)^{3-}$  and  $(\text{PO}_4)^{3-}$  bending (600–100  $\text{cm}^{-1}$ ) regions.

#### Hydroxyl-stretching region

Infrared and Raman spectra of the hydroxyl-stretching region of conichalcite are shown in Fig. 2. The results of the analyses of the spectra are given in Table 4 and compared with the study by Martens *et al.* (2003b), which reported Raman spectra for the adelite-group members austenite and a zincian conichalcite from Lorena mine, Cloncurry, Queensland, Australia. The most intense band at  $\sim 3150 \text{ cm}^{-1}$  both in IR and Raman spectra is characteristic of OH stretching. On either side of this, four symmetrical bands are located around 3300, 3250, 3050 and 2900  $\text{cm}^{-1}$ . However, the band positions and their intensities differ slightly. The differences in the band positions for this mineral are attributed to the changes in composition depending on the amount of Cu in the mineral. These observations agree with the chemistry and crystal structure of the

mineral of the adelite group (Hawthorne, 1976, 1990; Clark *et al.*, 1997; Kharisun *et al.*, 1998). Replacement of the Zn in austenite by the Cu in conichalcite causes a shift of the 3250  $\text{cm}^{-1}$  band of austenite to the lower wavenumber of 3125  $\text{cm}^{-1}$  (see Table 4).

Figure 3 shows the MIR region 2200–1200  $\text{cm}^{-1}$  where hydroxyl deformation modes of water are found at  $\sim 1600 \text{ cm}^{-1}$  and overtones of phosphate and arsenate ions appeared around 2000 and 1400  $\text{cm}^{-1}$ . Minerals containing physically adsorbed water give rise to strong bands at 3450  $\text{cm}^{-1}$ , the water hydroxyl-stretching vibration, and at  $\sim 1600 \text{ cm}^{-1}$ , the water-bonding vibrations (Frost *et al.*, 1998, 2003a; Martens *et al.*, 2004). In the present sample, two well resolved bands at 1644 and 1823  $\text{cm}^{-1}$  are indicative of chemically bonded water in the mineral. One strong band centred at 2079  $\text{cm}^{-1}$  may be an overtone of the antisymmetric mode of the  $\text{PO}_4^{3-}$  ion ( $\nu_3$ ). The low-wavenumber bands from 1300 to 1500  $\text{cm}^{-1}$  show structure both in IR and Raman and may be attributed to overtones of the arsenate ion.

TABLE 3. Vibrational analysis of the lattice modes in conichalcite.

Site	Crystal	Translational	Total
$C_1$	$D_2$		
$18A$	$18A$ $18B_1$ $18B_2$ $18B_3$	$B_1$ $B_2$ $B_3$	$18A$ $17B_1$ $17B_2$ $17B_3$

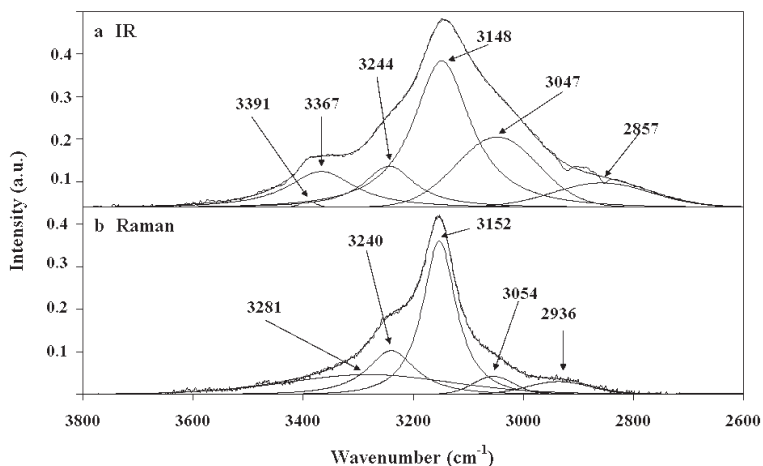


FIG. 2. Raman and IR spectra of conichalcite in the OH-stretching region.

TABLE 4. Raman and IR spectroscopic data ( $\text{cm}^{-1}$ ) of selected arsenate minerals.

Conichalcite* $\text{CaCu}^{2+}(\text{AsO}_4)(\text{PO}_4)(\text{OH})$		Conichalcite† $\text{CaCu}^{2+}(\text{AsO}_4)(\text{OH})$		Austinite $\text{CaZn}(\text{AsO}_4)(\text{OH})$
IR	<u>This work</u> Raman	<u>Published</u> Raman		<u>Published</u> Raman
3391				
3367s	3281			
3244	3240s	3233		3350
3148m	3152m	3158		3265
3047s	3054w	3086		
2857	2936s			
2079m	2077w			
2023s	2077			
1867				
1823m				
1776s				
1644w	1600m			
1468s	1523s			
1455c				
1414c				
1377c				
1361m	1335m			
1312s				
1164				
1100s				
1060s				
1052m	1050vw			
1040c				
1020s				
962c	955vw			
931m	911vw			
902c				
888w	869w			
841c	847w			
814w	834m	832		911

## CHARACTERIZATION OF CONICALCALCITE

TABLE 4. (contd.)

Conichalcite* CaCu <sup>2+</sup> (AsO <sub>4</sub> )(PO <sub>4</sub> )(OH)		Conichalcite <sup>†</sup> CaCu <sup>2+</sup> (AsO <sub>4</sub> )(OH)	Austinite <sup>‡</sup> CaZn(AsO <sub>4</sub> )(OH)
<u>This work</u>		<u>Published</u>	<u>Published</u>
IR	Raman	Raman	Raman
806c	822c	821	889
787w	812c	811	859
769c	780w	781	844
752m	754vw	750	818
693s			806
666w			738
573c			708
565m	538w		538
529c	534c	534	494
	486m	463	478
	450vw		457
	444m	446	420
	427s	430	
	364s	389	409
	358w	358	374
	335c	335	322
	324m	328	308
	287c	286	275
	276s	274	252
	221s		231
	206m	206	209
	198s	180	175
	178c	165	139
	162c	150	129
		123	

\* Conichalcite from the western part of Bagdad mine, Arizona (this work)

<sup>†</sup> Conichalcite from Lorena mine, Cloncurry, Queensland, Australia (Martens *et al.*, 2003)

<sup>‡</sup> Austinite from Lorena mine, Cloncurry, Queensland, Australia (Martens *et al.*, 2003)

Abbreviations of the bands character: m – major; s – shoulder; w – weak; vw – very weak; c – component

#### Arsenate and phosphate vibrations

The vibrational stretching in the 1200–530 cm<sup>-1</sup> region of conichalcite is shown in Fig. 4. The presence of AsO<sub>4</sub><sup>3-</sup> and PO<sub>4</sub><sup>3-</sup> bands are identified in this region. The Raman spectrum displays two weak bands at ~950 cm<sup>-1</sup>; but are strong in the IR spectrum at 962, 931 and 902 cm<sup>-1</sup>. This group of bands is attributed to the hydroxyl-stretching deformation modes of OH bonded to Ca or Cu. Sumin De Portilla (1974) also suggested that bands observed at 980 and 1010 cm<sup>-1</sup> are due to hydroxyl deformation modes. A previous study showed that the ν<sub>1</sub>(A<sub>1</sub>) and ν<sub>3</sub>(T<sub>2</sub>) modes of the free arsenate ion bands are at 837 and 878 cm<sup>-1</sup> in the Raman spectrum

(Griffith, 1970). The major Raman band at 834 cm<sup>-1</sup> and its components at 822 and 812 cm<sup>-1</sup> are assigned to the AsO<sub>4</sub><sup>3-</sup> symmetric stretching vibrations (ν<sub>1</sub>). The ν<sub>1</sub> mode is also activated fairly well in IR at 841 cm<sup>-1</sup>. The ν<sub>3</sub>(F<sub>2</sub>) mode is active both in IR and Raman. It is observed as a weak band at 780 cm<sup>-1</sup> in Raman but it is strong in IR, located at 752 cm<sup>-1</sup>, with components at 769, 787 and 806 cm<sup>-1</sup>. Raman spectra of the phosphate oxyanions in an aqueous system show a symmetric stretching mode (ν<sub>1</sub>) at 938 cm<sup>-1</sup>, the antisymmetric mode (ν<sub>3</sub>) at 1017 cm<sup>-1</sup>, the symmetric bending mode (ν<sub>2</sub>) at 420 cm<sup>-1</sup> and the ν<sub>4</sub> mode at 567 cm<sup>-1</sup> (Farmer, 1974). The major band in IR at 1052 cm<sup>-1</sup> with

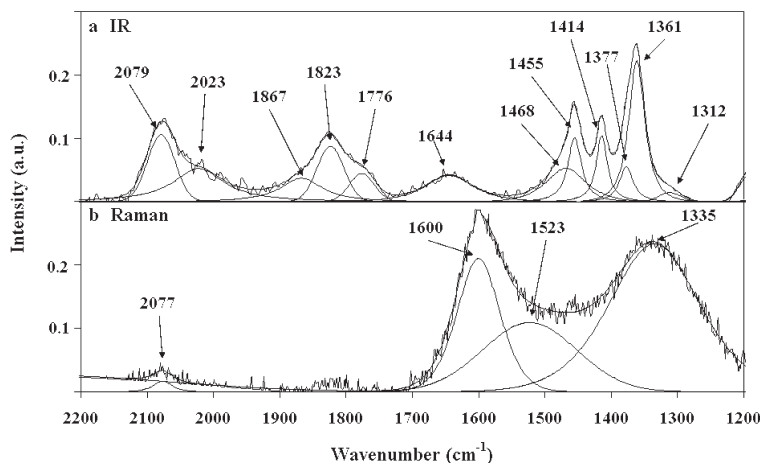


FIG. 3. Raman and IR spectra of conichalcite in the 2200–1200  $\text{cm}^{-1}$  region.

three shoulders and a component at 1100, 1060, 1020 and 1040  $\text{cm}^{-1}$  is identified as the  $\nu_3$  mode of the phosphate oxyanion. This complex band profile observed around 1052  $\text{cm}^{-1}$  is in excellent agreement with the complex band profile at  $\sim 1100 \text{ cm}^{-1}$  in a number of natural zinc phosphate minerals (Frost, 2004a). But this mode is weak in the Raman spectrum at 1050  $\text{cm}^{-1}$ . The reason might be a low concentration of phosphate ion partially substituted by an arsenate ion in the present conichalcite sample. CuO-stretching vibrations were noticed in dufite of the adelite group at 549 and 512  $\text{cm}^{-1}$  (Martens *et al.*, 2003). The low-wavenumber bands of IR shown here at 573 and 565  $\text{cm}^{-1}$  are assigned to CuO-stretching vibrations.

#### Low-wavenumber region (600–100 $\text{cm}^{-1}$ )

Farmer (1974) reported the bending modes of the phosphate ion in autunites ( $\nu_4$ ) at 615 and 545  $\text{cm}^{-1}$ . The  $\text{PO}_4^{3-}$   $\nu_4$  mode was also observed by Raman spectra in saléeite, a mineral of uranyl phosphate at 612 and 573  $\text{cm}^{-1}$  (Frost and Weier, 2004a,b) and, for another aluminium phosphate mineral, augelite, for which at 635  $\text{cm}^{-1}$  an intense band with component bands at 643 and 615  $\text{cm}^{-1}$  (Frost and Weier, 2004c) was also recorded. The low-wavenumber region of the Raman spectrum of conichalcite is shown in Fig. 5. Two Raman bands at 538 and 534  $\text{cm}^{-1}$  and an IR band at 529  $\text{cm}^{-1}$  are attributed to the  $\nu_4$  mode of  $\text{PO}_4^{3-}$ . The free  $\text{AsO}_4^{3-}$  ion exhibits  $\nu_2(\text{E})$  and  $\nu_4(\text{T}_2)$  modes at 349 and 463  $\text{cm}^{-1}$

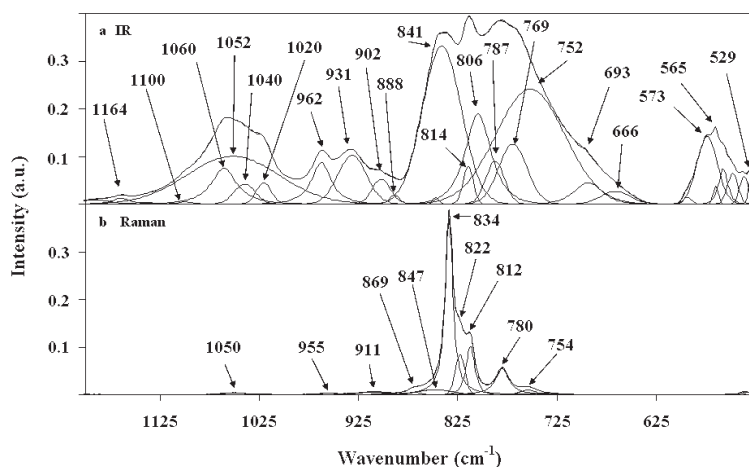


FIG. 4. Raman and IR spectra of conichalcite in the  $(\text{AsO}_4)^{3-}$  and  $(\text{PO}_4)^{3-}$ -stretching region.

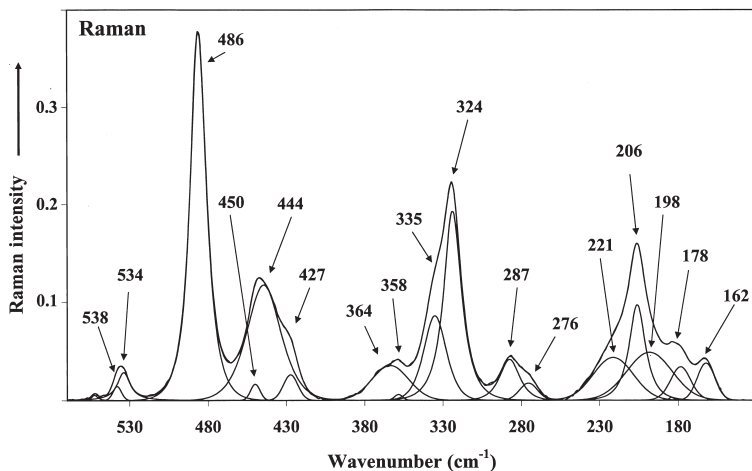


FIG. 5. Raman spectrum of the low wavenumber region ( $600\text{--}100\text{ cm}^{-1}$ ).

(Griffith, 1970). Conicalcalcite shows three intense groups of bands at  $\sim 500$ ,  $300$  and  $200\text{ cm}^{-1}$ . In the first group, the most intense band at  $486\text{ cm}^{-1}$  with a doublet at  $444$  and  $427\text{ cm}^{-1}$  is due to the splitting of the  $\nu_4(T_2)$  mode while the middle group dominated by a sharp peak at  $324\text{ cm}^{-1}$  but, with a number of component bands, is linked to the  $\nu_2$  bending-mode vibrations of  $(\text{AsO}_4)^{3-}$ . Two bands, at  $287$  and  $276\text{ cm}^{-1}$ , may be assigned to  $\text{OCuO}$ -bending modes. Other bands observed at  $206\text{ cm}^{-1}$  with components at  $198$ ,  $178$  and  $162\text{ cm}^{-1}$  can be described as lattice vibrations.

#### Electronic (reflectance) spectra

The electronic spectra of six-coordinated  $\text{Cu(II)}$  complexes are analysed assuming approximate  $4/mmm$  ( $D_{2h}$ ) or  $4mm$  ( $C_{4v}$ ) point symmetry for the  $\text{Cu}^{2+}$  ion and its ligands. The  $e_g$  and  $t_{2g}$  levels of the free ion term;  $^2D$  are further split into  $B_{1g}$ ,  $A_{1g}$ ,  $B_{2g}$  and  $E_g$  levels, respectively. Therefore, three spin-allowed transitions are expected for  $\text{Cu(II)}$  in the NIR and visible regions (Lever, 1984). The bands are resolved by Gaussian analysis and assigned to  $^2B_{1g} \rightarrow ^2A_{1g}$ ,  $^2B_{1g} \rightarrow ^2B_{2g}$  and  $^2B_{1g} \rightarrow ^2E_g$  transitions in order of increasing energy. The sequence of energy levels depends on the amount of distortion due to ligand field and Jahn-Teller effects (Ferguson *et al.*, 1975).

The electronic (reflectance) spectra of conicalcalcite (Fig. 6) show a very strong band centred at  $\sim 10,000\text{--}7000\text{ cm}^{-1}$  with a well defined

shoulder at  $11,000\text{--}10,000\text{ cm}^{-1}$  in the high-energy NIR region of  $11,000\text{--}6500\text{ cm}^{-1}$  (Fig. 6) and a broad feature in the visible spectrum centred at  $\sim 18,000\text{--}11,000\text{ nm}$ ; Fig. 6a). Near-IR reflectance spectroscopy has also been used to show the presence of water and hydroxyl units in the mineral. The spectrum in the NIR region,  $7000\text{--}4000\text{ cm}^{-1}$ , is shown in Fig. 7. Two bands at  $7060$  (Fig. 6b) and  $6452\text{ cm}^{-1}$  are attributed to the first overtone of the fundamental hydroxyl-stretch mode. The other two main bands at  $6000\text{--}5000\text{ cm}^{-1}$  are assigned to water-combination modes of the hydroxyl fundamentals of water. The sharp band located at  $4143\text{ cm}^{-1}$  with structure is assigned to the combination of the stretching and deformation modes of the  $M\text{-OH}$  units of conicalcalcite (Frost and Erickson, 2005).

The three broad intense spin-allowed d-d transitions of  $\text{Cu(II)}$  in the present mineral are identical with  $\lambda_{\text{max}}$  differently centered for several  $\text{Cu(II)}$  complex compounds (Hathaway and Billing, 1970; Hathaway, 1984; Reddy *et al.*, 1987; Ciobanu *et al.*, 2003; Reddy *et al.*, 2004) in tetragonally distorted octahedral coordination. As shown in the Fig. 6, conicalcalcite displays three bands. The first band at  $10575\text{ cm}^{-1}$  shows an additional band at  $9280\text{ cm}^{-1}$ . The broad band is centred at  $8585\text{ cm}^{-1}$  with two components at  $8680$  and  $8000\text{ cm}^{-1}$ . The visible region band at  $13,965\text{ cm}^{-1}$  also splits into two with maxima at  $15,313$  and  $12,500\text{ cm}^{-1}$ . As expected, the three spin-allowed bands are broad and intense. The Gaussian band-fitting shows further splitting. The

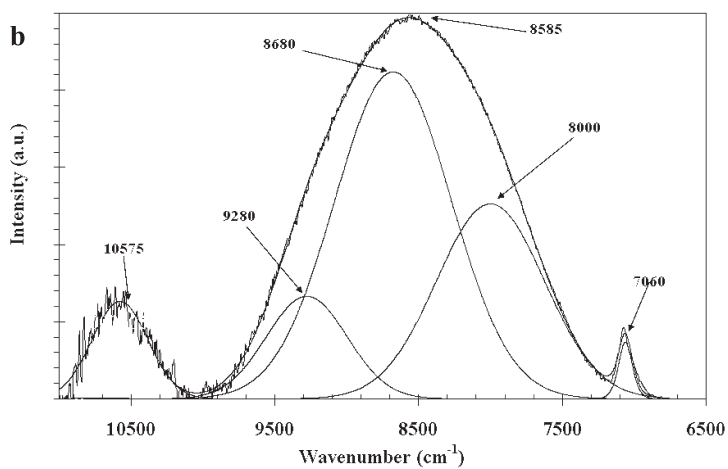
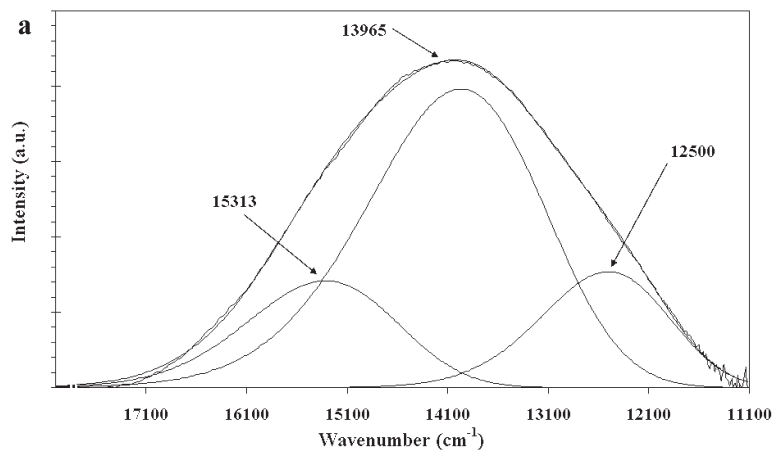


FIG. 6. Electronic spectra of conichalcite: (a) visible region; (b) NIR region.

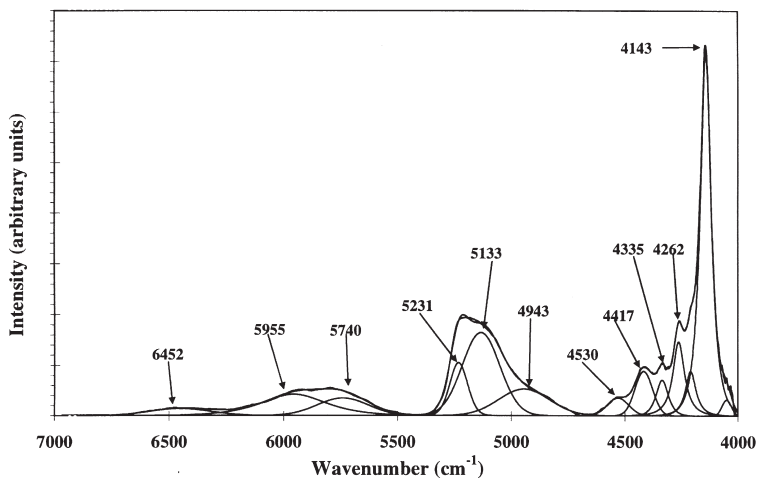


FIG. 7. NIR spectrum of conichalcite in the 4000 to 7000  $\text{cm}^{-1}$  region.

TABLE 5. Comparison of octahedral and tetragonal field parameters ( $\text{cm}^{-1}$ ) of  $\text{Cu}^{2+}$  in selected minerals.

Mineral	Dq	Ds	Dt	Reference
Brochantite [ $\text{Cu}_4^{2+}(\text{SO}_4)(\text{OH})_6$ ]	1050	1730	285	Reddy <i>et al.</i> (1987)
Connellite [ $\text{Cu}_{36}^{2+}\text{Cl}_6(\text{SO}_4)_2(\text{OH})_{62}\cdot 12\text{H}_2\text{O}$ ]	1205	1525	450	Sreeramulu <i>et al.</i> (1990)
Cornetite [ $\text{Cu}_3^{2+}(\text{PO}_4)(\text{OH})_3$ ]	1257	1434	380	Venkateramaiah <i>et al.</i> (1996)
Chrysocolla [ $\text{Cu}^{2+}, \text{Al}$ ] <sub>2</sub> $\text{H}_2\text{Si}_2\text{O}_5(\text{OH})_4\cdot n\text{H}_2\text{O}$ ]	1063	1697	268	Ravikumar <i>et al.</i> (1998)
Smithsonite [(Zn, $\text{Cu}^{2+}$ )( $\text{CO}_3$ )]	1250	1770	338	Reddy <i>et al.</i> (2004)
Conichalcite [ $\text{CaCu}^{2+}(\text{ASO}_4)(\text{OH})$ ]	1058	1711	348	This work

assignments of the bands are made as follows:

$${}^2\text{B}_{1g} \rightarrow {}^2\text{A}_{1g} = 4\text{Ds} + 5\text{Dt} = 8585 \text{ cm}^{-1}$$

$${}^2\text{B}_{1g} \rightarrow {}^2\text{B}_{2g} = 10\text{Dq} = 10,575 \text{ cm}^{-1}$$

$${}^2\text{B}_{1g} \rightarrow {}^2\text{E}_g = 10\text{Dq} + 3\text{Ds} - 5\text{Dt} = 13,965 \text{ cm}^{-1}$$

The crystal field (Dq) and tetragonal field (Ds and Dt) parameters derived from the observed data are  $\text{Dq} = 1058$   $\text{Ds} = 1711$  and  $\text{Dt} = 348\text{cm}^{-1}$ . The values of Dq and Dt in tetragonal field will have the same sign for an axial elongation and opposite sign if Cu(II) experiences axial compression (Hathaway and Billing, 1970). The same sign of Dq and Dt values confirms Cu(II) symmetry distortion from octahedral to elongated tetragonal field in conichalcite. The crystal field and tetragonal field parameters of Cu(II) derived from the electronic spectra of conichalcite agree well with the values reported for other tetragonal distorted octahedral  $\text{Cu}^{2+}$  complexes (Table 5).

## Conclusions

Electronic and vibrational spectroscopic data are reported for the mineral conichalcite. The presence of a phosphate ion as an impurity was found in the mineral by EDX analyses and reflected by the  $\nu_3$  and  $\nu_4$  modes of  $\text{PO}_4^{3-}$  in both the IR and Raman spectra. The presence of water and hydroxyl units in the mineral was found from spectral features observed in both IR and NIR spectra. Substitution of the Cu in conichalcite for the Zn in austinite causes a shift of bands to lower wavenumbers. The three spin-allowed electronic bands of Cu(II) are consistent with

tetragonally elongated coordination of the Cu polyhedra.

## Acknowledgements

The financial and infra-structure support of the Queensland University of Technology (QUT), Inorganic Materials Research Program is gratefully acknowledged. We thank the Australian Research council (ARC) for funding the research work. Two of the authors; B.J. Reddy and W. Martens are grateful to the Queensland University of Technology for the award of a Visiting Fellowship and an ARC Post-doctoral fellowship of QUT, respectively.

## References

- Burns, R.G. (1970) *Mineralogical Applications of Crystal Field Theory*. Earth Sciences Series, Cambridge University Press, Cambridge, UK, 224 pp.
- Ciobanu, A., Zalaru, F., Zalaru, C., Dumitrascu, F. and Draghici, C. (2003) Coordination compounds of Cu(II) with Schiff bases derived from formylmenthone and aromatic amines. *Acta Chimica Slovenica*, **50**, 441–450.
- Clark, L.A., Pluth, J.J., Steele, I., Smith, J.V. and Sutton, S.R. (1997) Crystal structure of austinite,  $\text{CaZn}(\text{AsO}_4)\text{OH}$ . *Mineralogical Magazine*, **61**, 677–683.
- Farmer, V.C. (1974) *The Infrared Spectra of Minerals*. Monograph **4**, Mineralogical Society, 539 pp.
- Ferguson, J., Wood, T.E. and Guggenheim, H.J. (1975)

- Electronic absorption spectra of tetragonal and pseudotetragonal cobalt(II). I. Dipotassium tetrafluorocobaltate, dirubidium tetrafluorocobaltate, dipotassium magnesium tetrafluorocobaltate, and dirubidium magnesium tetrafluorocobaltate. *Inorganic Chemistry*, **14**, 177–183.
- Frost, R.L. (2004a) An infrared and Raman spectroscopic study of natural zinc phosphates. *Spectrochimica Acta, Part A: Molecular and Biomolecular Spectroscopy*, **60A**, 1439–1445.
- Frost, R.L. (2004b) An infrared and Raman spectroscopic study of the uranyl micas. *Spectrochimica Acta, Part A, Molecular and Biomolecular Spectroscopy*, **60**, 1469–1480.
- Frost, R.L. and Erickson, K.L. (2005) Near-infrared spectroscopic study of selected hydrated hydroxylated phosphates. *Spectrochimica Acta, Part A: Molecular and Biomolecular Spectroscopy*, **61**, 45–50.
- Frost, R.L. and Weier, M. (2004a) Raman microscopy of autunite minerals at liquid nitrogen temperature. *Spectrochimica Acta, Part A: Molecular and Biomolecular Spectroscopy*, **60**, 2399–2409.
- Frost, R.L. and Weier, M. (2004b) Raman microscopy of selected autunite minerals. *Neues Jahrbuch für Mineralogie, Monatshefte*, 575–594.
- Frost, R.L. and Weier, M.L. (2004c) Vibrational spectroscopy of natural augelite. *Journal of Molecular Structure*, **697**, 207–211.
- Frost, R.L., Kristof, J., Paroz, G.N., Tran, T.H. and Klopogge, J.T. (1998) The role of water in the intercalation of kaolinite with potassium acetate. *Journal of Colloid and Interface Science*, **204**, 227–236.
- Frost, R.L., Martens, W.N. and Williams, P.A. (2002) Raman spectroscopy of the phase-related basic copper arsenate minerals olivenite, cornwallite, cornubite and clinoclase. *Journal of Raman Spectroscopy*, **33**, 475–484.
- Frost, R.L., Martens, W., Ding, Z., Klopogge, J.T. and Johnson, T.E. (2003a) The role of water in synthesised hydrotalcites of formula  $Mg_xZn_{6-x}Cr_2(OH)_{16}(CO_3) \cdot 4H_2O$  and  $Ni_xCo_{6-x}Cr_2(OH)_{16}(CO_3) \cdot 4H_2O$  – an infrared spectroscopic study. *Spectrochimica Acta, Part A: Molecular and Biomolecular Spectroscopy*, **59A**, 291–302.
- Frost, R.L., Martens, W., Williams, P.A. and Klopogge, J.T. (2003b) Raman spectroscopic study of the vivianite arsenate minerals. *Journal of Raman Spectroscopy*, **34**, 751–759.
- Frost, R.L., Klopogge, J.T. and Martens, W.N. (2004) Raman spectroscopy of the arsenates and sulphates of the tsumcorite mineral group. *Journal of Raman Spectroscopy*, **35**, 28–35.
- Griffith, W.P. (1970) Raman studies on rock-forming minerals. II. Minerals containing  $MO_3$ ,  $MO_4$ , and  $MO_6$  groups. *Journal of the Chemical Society [Section] A: Inorganic, Physical, Theoretical*, 286–291.
- Hathaway, B.J. (1984) A new look at the stereochemistry and electronic properties of complexes of the copper(II) ion. *Structure and Bonding (Berlin, Germany)*, **57 (Complex Chemistry)**, 55–118.
- Hathaway, B.J. and Billing, D.E. (1970) Electronic properties and stereochemistry of mononuclear complexes of the copper(II) ion. *Coordination Chemistry Reviews*, **5**, 143–207.
- Hawthorne, F.C. (1976) A refinement of the crystal structure of adamite. *The Canadian Mineralogist*, **14**, 143–148.
- Hawthorne, F.C. (1990) Structural hierarchy in  $M[6]T[4].vphi.n$  minerals. *Zeitschrift Kristallographie*, **192**, 1–52.
- Jambor, J.L., Owens, D.R. and Dutrizac, J.E. (1980) Solid solution in the adelite group of arsenates. *The Canadian Mineralogist*, **18**, 191–195.
- Keller, P., Hess, H. and Dunn, P.J. (1981) Jamesite,  $Pb_2Zn_2Fe_5^{3+}O_4(AsO_4)_5$ , a new mineral from Tsumeb, Namibia. *Chemie der Erde*, **40**, 105–109.
- Keller, P., Hess, H. and Dunn, P.J. (1982) Johillerite,  $Na(Mg, Zn)_3Cu(AsO_4)_3$ , a new mineral from Tsumeb, Namibia. *Tschermaks Mineralogische und Petrographische Mitteilungen*, **29**, 169–175.
- Kharisun, Taylor, M.R., Bevan, D.J.M. and Pring, A. (1998) The crystal chemistry of duftite,  $PbCuAsO_4(OH)$  and the  $\beta$ -duftite problem. *Mineralogical Magazine*, **62**, 121–130.
- Lever, A.B.P. (1984) *Studies in Physical and Theoretical Chemistry*, 2<sup>nd</sup> edition. Vol. 33, Inorganic Electronic Spectroscopy, Elsevier, Amsterdam, 862 pp.
- Martens, W., Frost, R.L. and Klopogge, J.T. (2003a) Raman spectroscopy of synthetic erythrite, partially dehydrated erythrite and hydrothermally synthesized dehydrated erythrite. *Journal of Raman Spectroscopy*, **34**, 90–95.
- Martens, W., Frost, R.L. and Williams, P.A. (2003b) Molecular structure of the adelite group of minerals – a Raman spectroscopic study. *Journal of Raman Spectroscopy*, **34**, 104–111.
- Martens, W.N., Frost, R.L., Klopogge, J.T. and Williams, P.A. (2003c) The basic copper arsenate minerals olivenite, cornubite, cornwallite, and clinoclase: An infrared emission and Raman spectroscopic study. *American Mineralogist*, **88**, 501–508.
- Martens, W.N., Klopogge, J.T., Frost, R.L. and Rintoul, L. (2004) Single-crystal Raman study of erythrite,  $Co_3(AsO_4)_2 \cdot 8H_2O$ . *Journal of Raman Spectroscopy*, **35**, 208–216.
- Qurashi, M.M. and Barnes, W.H. (1963) Structures of the minerals of the descloizite and adelite groups. IV.

## CHARACTERIZATION OF CONICALCALCITE

- Descloizite and conicalcalcite. 2. Structure of conicalcalcite. *The Canadian Mineralogist*, **7**, 561–77.
- Radcliffe, D. and Simmons, W.B., Jr. (1971) Austinite. Chemical and physical properties in relation to conicalcalcite. *American Mineralogist*, **56**, 1357–1363.
- Ramanaiah, M.V., Ravikumar, R.V.S.S.N., Srinivasulu, G., Reddy, B.J. and Rao, P.S. (1996) Detailed spectroscopic studies on cornetite from Southern Shaba, Zaire. *Ferroelectrics*, **175**, 175–182.
- Ravikumar, R.V.S.S.N., Madhu, N., Chandrasekhar, A.V., Reddy, B.J., Reddy, Y.P. and Rao, P.S. (1998) Cu(II), Mn(II) in tetragonal site in chrysocolla. *Radiation Effects and Defects in Solids*, **143**, 263–272.
- Reddy, B.J., Yamauchi, J., Ravikumar, R.V.S.S.N., Chandrasekhar, A.V. and Venkataramanaiah, M. (2004) Optical and EPR investigations on smithsonite minerals. *Radiation Effects and Defects in Solids*, **159**(3), 141–147.
- Reddy, K.M., Jacob, A.S., Reddy, B.J. and Reddy, Y.P. (1987) Optical absorption spectra of copper(2+) in brochantite. *Physica Status Solidi B: Basic Research*, **139**(2), K145–K150.
- Sreeramulu, P., Reddy, K.M., Jacob, A.S. and Reddy, B.J. (1990) UV-VIS, NIR, IR, and EPR spectra of connellite. *Journal of Crystallographic and Spectroscopic Research*, **20**, 93–96.
- Sumin De Portilla, V.I. (1974) Infrared spectroscopic investigation of the structure of some natural arsenates and the nature of hydrogen-bonds in their structures. *The Canadian Mineralogist*, **12**, 262–268.
- Taggart, J.E., Jr. and Foord, E.E. (1980) Conicalcalcite, cuprian austinite, and plumboan conicalcalcite from La Plata County, Colorado [USA]. *Mineralogical Record*, **11**, 37–38.

[Manuscript received 19 August 2004:  
revised 2 March 2005]